M. L. Joshi
S. Dash

# Dislocation-Induced Deviation of Phosphorus-Diffusion Profiles in Silicon

**Abstract:** Deviation of phosphorus-impurity profiles in silicon from ideal ones under the diffusion condition of high surface concentrations is well known. Diffusion of high concentrations of phosphorus is also known to cause generation of dislocations with edge character in silicon wafer surfaces. A major cause of the deviation of the phosphorus profile is shown to be solute accumulation at these dislocations. The dislocation-precipitated profile is calculated for the ideal complementary error-function diffusion profile of phosphorus with $10^{21}$ atoms/cm$^3$ of surface concentration, using Ham's model of stress-assisted precipitation on dislocations. The results are shown to account for most of the major features of the experimental diffusion profiles.

## Introduction

Diffusion profiles in silicon are known to deviate considerably from the theoretically expected complementary error function (for constant solute concentration source) under the conditions of high surface concentration and shallow diffusion.[1-3] Various reasons may be advocated for this phenomenon. These include (1) concentration dependence of diffusivity,[2] (2) state of ionization of the impurity, (3) effect of the built-in electric field,[4] (4) time needed to reach a constant-source condition at the glass-silicon interface, (5) movement of the surface during diffusion caused by silicon oxidation, (6) solute precipitation,[1] and (7) dislocations created during diffusion or existing before diffusion.

Tannenbaum's phosphorus profiles obtained by diffusion from a constant source in single-crystal silicon wafers are well known.[1] These profiles were measured by using both the electrical and radio-tracer techniques. Our own measurements, using the same techniques under almost the same diffusion conditions, are represented in Fig. 1; the pertinent diffusion conditions are given in the same figure. The major significant feature, as seen from both Tannenbaum's and our own phosphorus-distribution curves, is the existence of a large difference between the electrical and the radio-tracer profiles. This difference has been interpreted by Tannenbaum to be due either to precipitation of phosphorus or to the decrease in the electron mobility; however, Tannenbaum favors the former interpretation.

Since the diffusion of high concentrations of phosphorus is known to induce dislocations in silicon, the dislocations may be considered to be important sites for precipitation. Phosphorus precipitated along dislocations would become electrically inactive. This phenomenon, if it is real, may explain the large difference between the two profiles in Fig. 1. Researchers have often speculated about this effect of dislocations on the impurity profiles in silicon. However, no attempt seems to have been made yet to apply the dislocation precipitation model in a quantitative manner to the silicon diffusion profiles. The intent of this paper is to examine quantitatively the effect of the diffusion-induced dislocations on the diffusion of high concentrations of phosphorus. The various other reasons that have been advocated for the deviation of diffusion profiles (under conditions of high surface concentration) will be neglected for the purpose of the dislocation model.

Before proceeding to investigate the effect of dislocation precipitation in detail, it is necessary to make clear the significance of the electrical profile in Fig. 1. It should be understood that this profile represents the total (and not only the ionized) impurity concentration. Irvin's standard curves[5] of resistivity versus impurity concentrations were used for the profile determination. Those curves are based upon measurements in uniformly doped crystals, and the measurements are direct wherever possible—radiotracer, calorimetric, and densitometric. Consequently, the electrical profile automatically takes into account percent ionization, impurity band conduction, and the possible precipitation in bulk-doped crystals. The dislocation-precipitation effect, however, will not be seen from the electrical measurements because Irvin's curves refer to the concentrations in uniformly-doped crystals. Dislocations are created only when impurity gradients exist—that is, only during diffusion. The ratio-tracer profile includes both the *total* phosphorus (as represented by the electrical measurements) and the dislocation-precipitation.

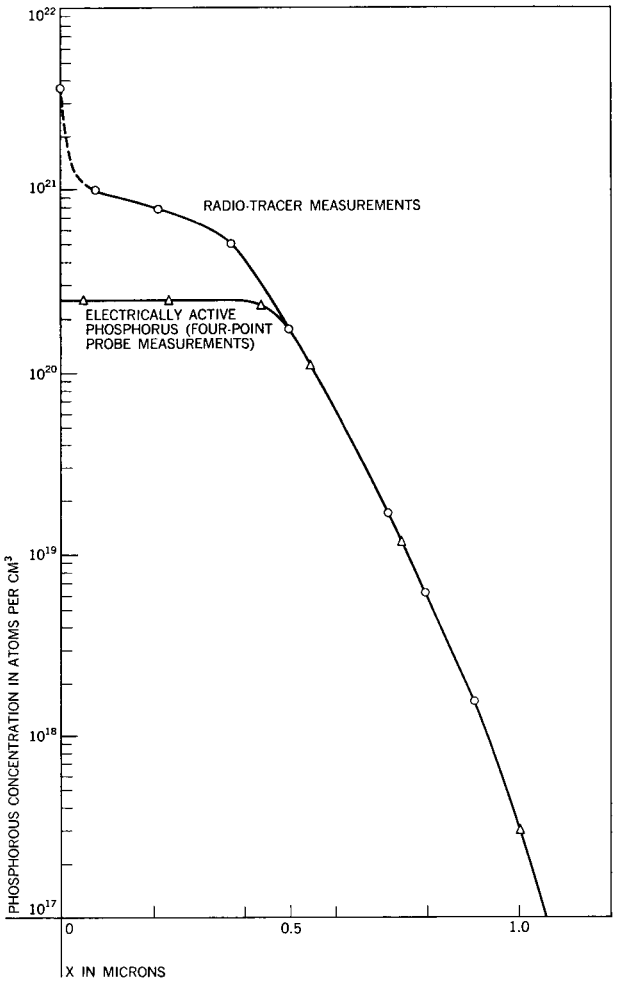


**Figure 1** Diffusion profiles of phosphorus in silicon; comparison of the distribution obtained by radio-tracer measurements (total phosphorus, see also Kooi[10]) with that obtained by resistivity measurements (electrically active phosphorus). Both sets of measurements were obtained from two samples identically diffused for 16 min. at 1050°C; open-tube diffusion from a $P_2O_5$ diffusion source.

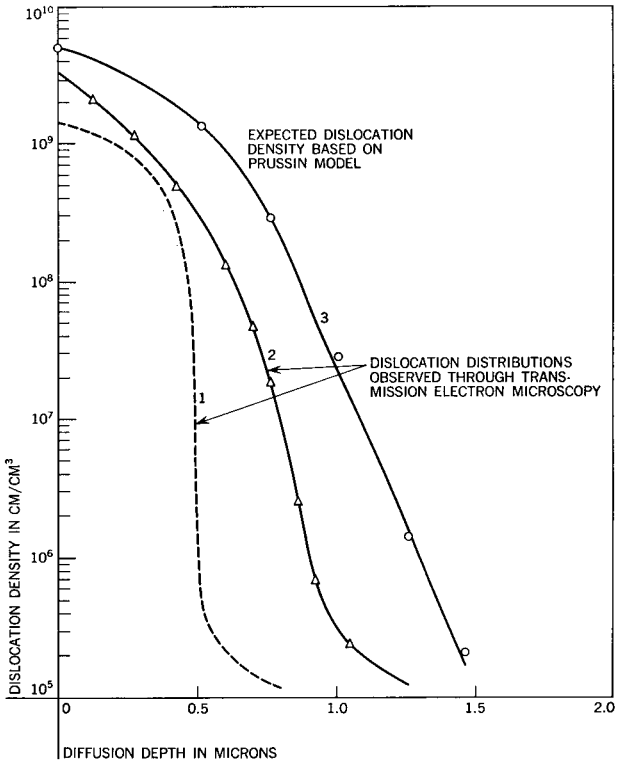


**Figure 2** Experimental dislocation distributions for phosphorus diffusion ($C_s > 10^{21}$ atoms/cm$^2$) to a depth of about $2\mu$ in a silicon wafer.

It is well established that at high concentrations of phosphorus ($C_s > 10^{21}$ atoms/cm$^3$) diffusion introduces dislocation networks having a density of about $5 \times 10^9$ cm/cm$^3$ at the surface.[6] The network density decreases rapidly with penetration and merges into the background dislocation density at a depth of about $\frac{1}{2}\mu$. Figure 2 shows the dislocation distributions, determined experimentally by electron microscopy[6] and by chemical techniques, for the diffusion conditions given in Fig. 1. There exists a variation in the dislocation distribution from wafer to wafer and the curves 1 and 2 in Fig. 2 represent the upper and lower limit, respectively, of these variations.

According to Prussin's theory[7] of diffusion-induced misfit dislocations, the dislocations would be expected to travel much deeper towards the junction. The anchoring forces due to the formation of nodes and solute pinning, however, cause shallower penetration of dislocations generated at the surface early in the diffusion. The generation of dislocations as indicated by slip line structures is found to begin with a phosphorus surface concentration as small as $2 \times 10^{20}$ atoms/cm$^3$, measured electrically. This would imply that the effect of dislocations, if any, on the diffusion profiles would be seen first at this surface concentration and become more evident at high concentrations.

The diffusion-induced dislocations have predominant edge character and consequently, under the conditions of supersaturation, phosphorus atoms can be expected to precipitate along the dislocations and at other strain centers in the silicon matrix. Electron microscopy gives evidence of both general precipitation in the matrix and at the dislocations.[7] Figure 3 is a transmission electron micrograph representing extensive precipitation on the diffusion-induced dislocation lines in a phosphorus-diffused silicon wafer. Although the usually observed dislocation precipitation is not as high as seen in Fig. 3, the evidence is

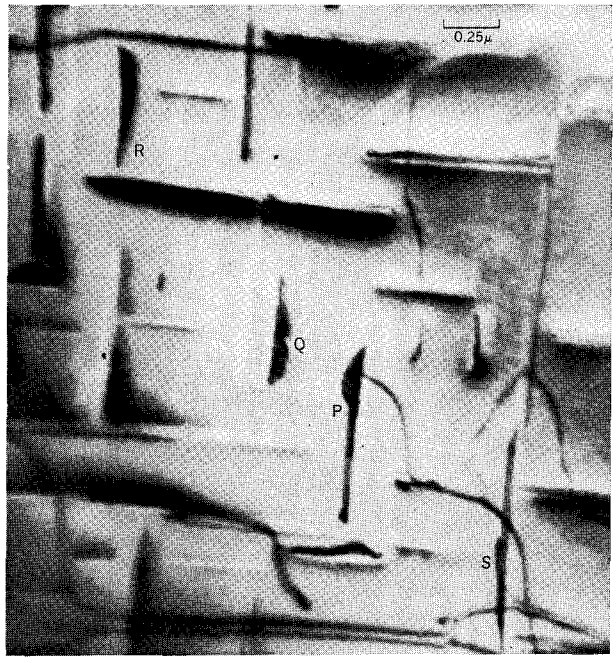


**Figure 3** Transmission electron micrograph showing profuse precipitation at diffusion induced dislocations P, Q and R in a ⟨100⟩ oriented silicon. White contrast lines are ridges from which dislocations have escaped.

**Figure 4** Resistivity as a function of net donor concentration. The circles are the compiled data of Irvin.[5] At concentrations about $6 \times 10^{19}$ cm$^{-3}$ it is generally assumed that the mobility $\mu = 75$ cm$^2$/volt-sec, given a straight line extrapolated to $8 \times 10^{20}$ cm$^{-3}$ at $\rho = 10^{-4}\Omega$-cm, on this plot. The dots are the result of calculating values of the mobility which force the distribution obtained from resistivity measurements to agree with that obtained from the tracer measurements. The inset shows the divergence of the two concentration determinations at high concentrations. The abscissa of the inset is the same as that of the graph (Tannenbaum's data).

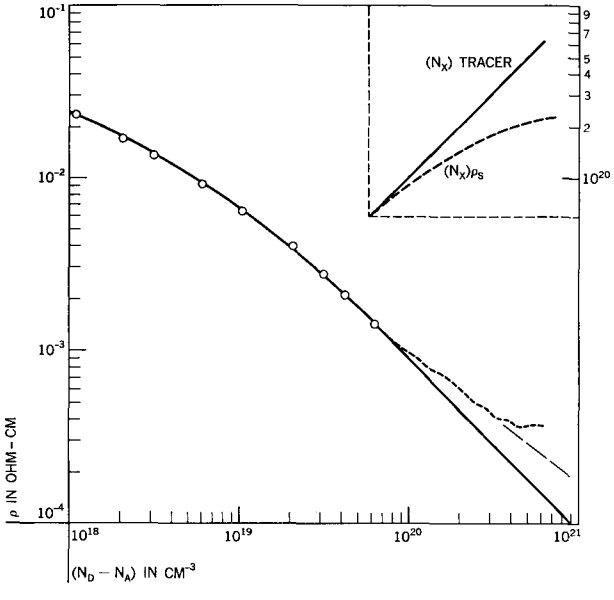


strong enough to indicate that dislocations are a major factor in causing diffusion profiles of phosphorus to deviate from those expected.

## Theory

- *Dislocation precipitation*

We will assume that the dislocations cause only a redistribution of the solute and do not involve any change in the flux entering the surface of a silicon wafer if the wafer is held at a given diffusion temperature under constant impurity concentration. This means that the area under the profile, $\int_0^{x_j} C(x, t)\, dx$, is unaltered by the presence of dislocations. (In the above expression $C(x, t)$ is the impurity concentration, which is a function of time $t$ and distance $x$, and $x_j$ is the junction depth.)

The solid solubility of phosphorus in silicon at 1050°C according to Trumbore[8] is $\approx 1 \times 10^{21}$ atoms/cm$^3$. Evidently there is supersaturation of phosphorus in the immediate neighborhood of the surface when the total surface concentration (i.e., that obtained by the radiotracer technique) exceeds the value of the solubility limit. The excess concentration of the impurity above this limit will be considered to be under the influence of the dislocation strain field. The value for solid solubility given by Trumbore, however, need not be regarded as the most accurate one. Since there exists a wide discrepancy in the values of solid solubility of phosphorus,[9] it was decided to use that particular value which can be inferred from Tannenbaum's curve of resistivity vs. donor concentration (Fig. 4). The point at which the electrical measurements begin to diverge from the radiotracer measurements in Fig. 4 has been regarded as the beginning of phosphorus precipitation. From this figure, we can infer that the most probable value for the solid solubility of phosphorus in silicon under the conditions of diffusion is about $10^{20}$ atoms/cm$^3$. This value is about half that found by Abrikosov et al.[11] in the Si-P system. We will use here a value of phosphorus solubility (at 1050°C) of $2 \times 10^{20}$ atoms/cm$^3$.

It is well-known that if a solute atom in a solid solution strains the crystal lattice appropriately, it will interact with the stress field of a dislocation.[12] Hence, in a supersaturated solution, the precipitation on dislocations may be significantly enhanced by stress-induced drift as compared with drift that would result solely from diffusion currents due to concentration gradients.

In the presence of both the stress field, characterized by an interaction energy $V(r)$, and gradients in the excess solute concentration $C_e(r, t)$, the solute current density is

$$J = D(\nabla C_e + C_e/kT \nabla V), \tag{1}$$

and

$$V(r, \theta) = -(A \sin \theta)/r, \tag{2}$$

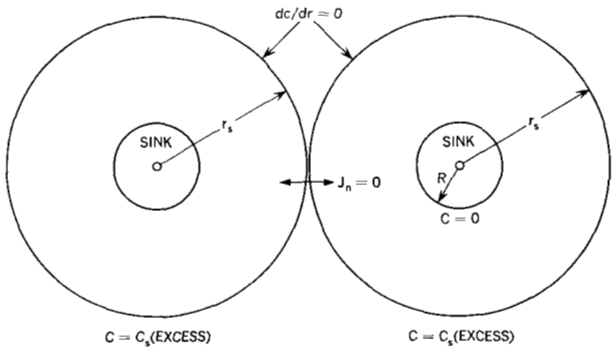


**Figure 5** Diffusion boundary conditions for dislocations which are treated as hollow cylinders.

for an edge dislocation. The terms $r$ and $\theta$ refer to cylindrical coordinates around the dislocation. Cottrell and Bilby[13] proposed that in the initial period of precipitation ($t \rightarrow 0$), $D \nabla C$ can be neglected. The condition $D \nabla C = 0$ is usually referred to as the drift approximation. Ham[14] re-examined the Cottrell-Bilby theory and has given a comprehensive analysis of stress-assisted precipitation on dislocations. He included a $D \nabla C$ term in his analysis.

In the model, a regular array of dislocations is first replaced by a single dislocation of "capture radius $R$" at the center of a cylinder of radius $r_s$, the original length of dislocation line per unit volume being

$$L = (\pi r_s^2)^{-1}. \tag{3}$$

This arrangement, with appropriate boundary conditions, is shown in Fig. 5. On the surface of the cylinder, the normal component of current density equals zero; that is, $J_n = 0$ at $r = r_s$. Taking into account the competition between dislocations, and also the gradient between $R$ and $r_s$, Ham shows that the time-dependence of the precipitated fraction, $W$, on dislocations is given by

$$W = 1 - \exp(-\lambda_0^2 Dt), \tag{4}$$

where

$$\lambda_0^2 \cong (2/r_s)^2[\ln(r_s/R) - (3/5)]^{-1}. \tag{5}$$

The precipitated concentration of the solute $C_p$ per unit volume is then calculated to be

$$C_p = W[\pi C_s(r_s^2 - R^2)]L. \tag{6}$$

Determination of the precipitation amount from Eqs. (4), (5) and (6) involves an estimate of the capture radius $R$. The value of $R$ is given by

$$R = [(Ae^{0.58})/(4kT)], \tag{7}$$

where

$$A = (3/\pi)Gba^3\epsilon, \tag{8}$$

with $G$ = shear modulus, $b$ = Burgers vector, $a$ = lattice parameter, and $\epsilon = \Delta r/r$, the atomic misfit parameter. Using $G = 7.6 \times 10^{11}$ dynes/cm$^2$, $a = 5.43$ Å, $\Delta r = 0.07$ for phosphorus, $r = 1.17$ Å, and $b = 3.84$ Å, $A = 25 \times 10^{-20}$ dynes-cm$^2$. For 1000°C, $R$ is then calculated to be about 60 Å. In iron,[14] where dislocation precipitation effects are significant, $R$ is about 14 Å. Therefore, for silicon, which has a more open lattice and a larger lattice parameter and Burgers vector, $R = 60$ Å seems reasonable. Assuming $R = 60$ Å, for different $r_s/R$ values (i.e., for different dislocation densities) $W$ vs. $(Dt)/r_s^2$ curves have been calculated, as shown in Fig. 6. It is difficult to establish the limits for the values of $R$ near its "true value." The true value may be as small as 30 Å since the effect of temperature was not taken into account in evaluating Eq. (8). On the other hand, there exists the possibility of coulombic attraction between dislocations acting as acceptors and the positively charged phosphorus ions. This effect could increase $R$. It is difficult, however, to assess this effect at the diffusion temperature in an almost degenerate extrinsic silicon. Therefore, it was decided to use $R = 60$ Å for the calculations of the dislocation-precipitated profiles $C_p(x)$.

- *Precipitation mechanism*

A necessary condition for precipitation in any two-component phase is that the phase must become thermodynamically unstable and tend to decompose into other phases. This requirement is usually accomplished by

**Figure 6** Time-dependent precipitated fraction, $W$, on dislocations as a function of $Dt/r_s^2$, obtained using Ham's model.

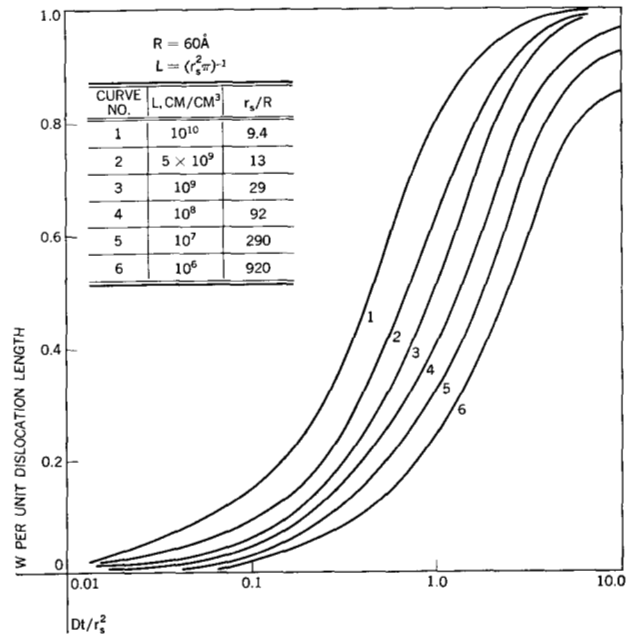

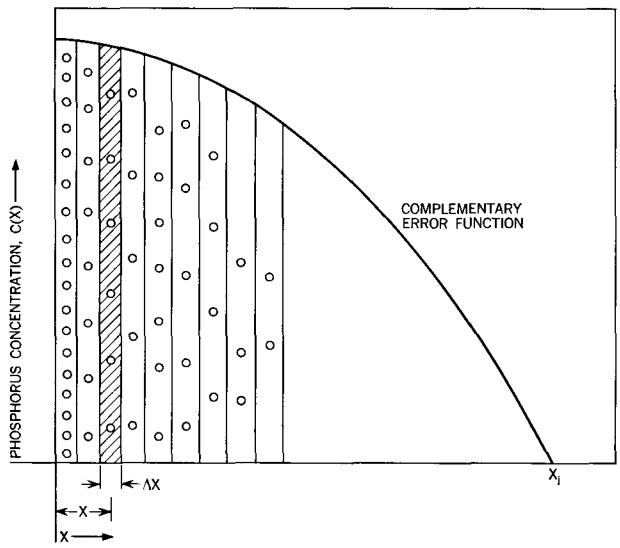


**Figure 7** Illustration of the method for calculating $C_p(x)$. Using Eq. (6), and assuming the dislocation concentration $L$ to be constant over any interval $\Delta x$, $C_p(x)$ can be calculated to give discrete values for each $\Delta x$-thick "slice" of the wafer. The number of dots shown in each slice is schematically proportional to $L$.

quenching. The dislocation precipitation as proposed here, however, is not according to this mechanism. It takes about 2 seconds or less in our experimental set-up for the diffused wafer to cool down from the diffusion temperature to 800°C, at which the atomic mobility almost vanishes. The precipitated fraction $W$ depends on the dimensionless parameter $Dt/r_s^2$ in Eq. (4) and consequently becomes negligibly small. A significant contribution toward dislocation precipitation would require very large values of $D$, about 500 times larger than the usual value of $D = 5 \times 10^{-13}$ cm$^2$/sec at 1050°C. While such high values are not ruled out, quenching experiments do not indicate any conclusive effect on the profiles. (In spite of these difficulties, we will calculate later the amount of precipitation involved during quenching, making some qualifying assumptions.) The precipitation mechanism we do assume to be operative is as follows.

The high state of strain introduced by diffusion of large amounts of phosphorus with considerable atomic misfit in silicon is responsible for producing dense misfit dislocations in the matrix during diffusion. Yield stresses of magnitude $>10^{10}$ dynes/cm$^2$ are generated. Such "cold-work" also introduces stored energy in the crystal. We have in our problem the two processes of cold-work and annealing operating simultaneously during the diffusion of high amounts of phosphorus. (It is well known that dislocations are generated when the surface concentrations correspond to the solid solubility limit.) The cold-worked matrix is expected to continuously adjust itself by thermally-activated self-diffusion. Solute atoms then will propagate to the dislocations or to other discrete strain centers and cause precipitation. This also means that the lattice during diffusion is not under true static equilibrium but is continuously working towards establishing equilibrium. During diffusion-anneal the strained lattice attempts to maintain in solution an impurity content of not more than the "solubility" limit, corresponding to the thermodynamic stability. This is exactly what is indicated by the value of $C_s$ (see Fig. 1) measured by electrical methods which do not measure the impurity that is out of solution; i.e., along dislocation lines.

With these considerations in mind, we will now investigate the practical consequences of dislocation precipitation through both of the mechanisms discussed above.

## Results

For the purpose of evaluating the dislocation-precipitated solute profiles under actual diffusion conditions, the following assumptions will be made:

(1) Dislocations do not become saturated.

(2) Solute atoms trapped by dislocations are removed from the main diffusion field.

(3) The dislocation distribution of curve 2 in Fig. 2, which was obtained experimentally, will be assumed to exist prior to diffusion (although in reality the dislocation dispersion in the interior of a wafer is also a time-dependent process).

(4) In the absence of dislocations, a strict complementary error function will be assumed as the solute profile. This function is given by

$$C = C_s[1 - \text{erfc}\,(x^2/4\,Dt)^{\frac{1}{2}}], \tag{9}$$

where

$C$ = solute concentration at $x$ and at time $t$,
$x$ = distance perpendicular to and from the wafer surface,
$C_s$ = constant surface concentration, and
$D$ = diffusivity.

(5) The precipitated amount will be calculated as illustrated in Fig. 7 for a thin slice $\Delta x$ at a depth $x$ in the diffusion profile, assuming a uniform concentration in the slice. Competition for solute between slices will be neglected.

- *Precipitation during diffusion*

With these assumptions, let us consider the effect of dislocation precipitation following the cold-work-anneal mechanism. Let us consider a hypothetical phosphorus diffusion having a complementary error function distribution (see curve 1, Fig. 8a) with the surface concentration $C_s = 10^{21}$ atoms/cm$^3$. Diffusivity will be taken to be concentration-independent and its value will be assumed to be

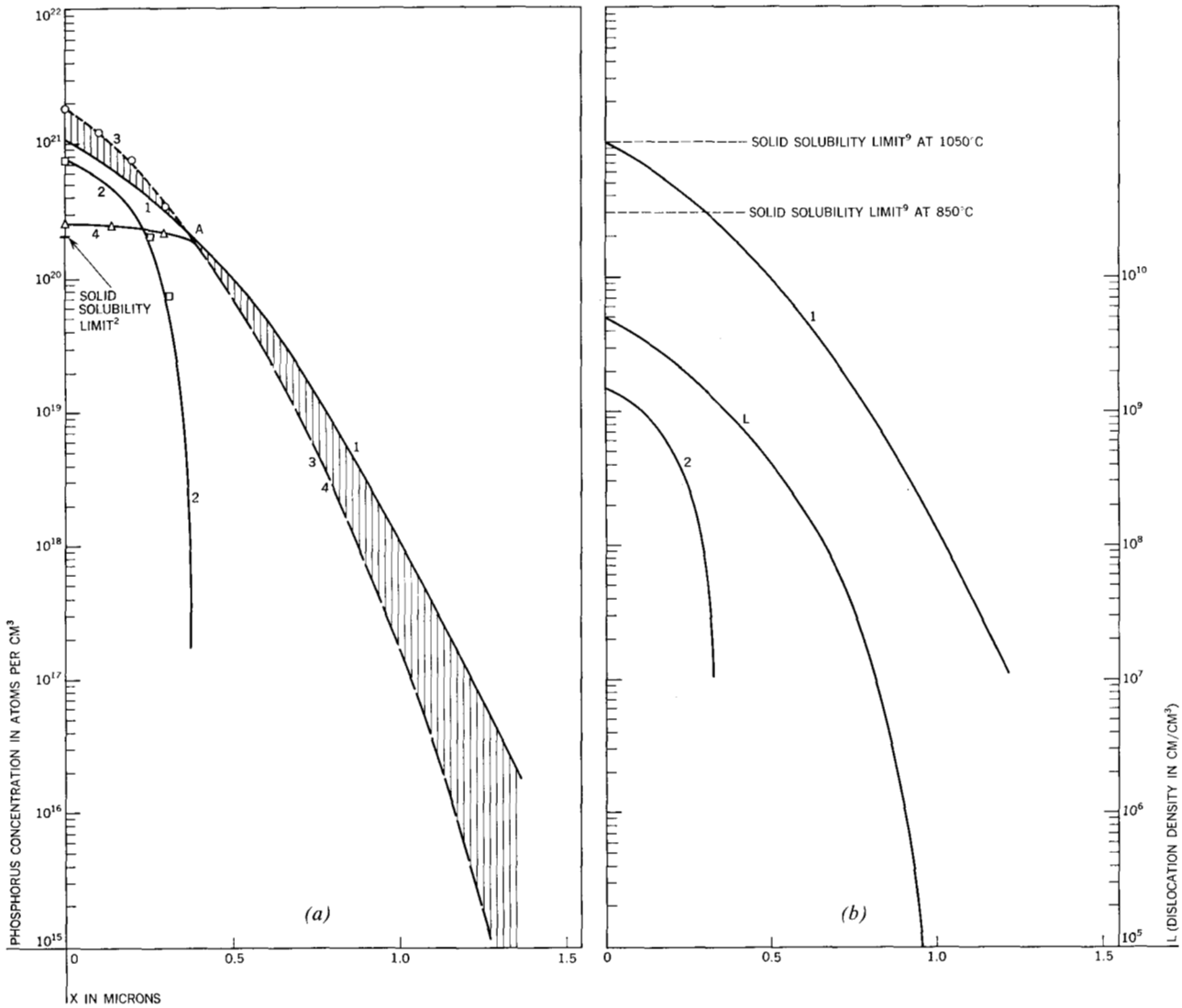


**Figure 8** Deviation of phosphorus-diffusion profiles from the expected (*erfc*) distribution. Diffusion is assumed to take place in highly intrinsic silicon (*n*-type, 50-Ω resistivity). $D = 5 \times 10^{-13}$ cm²/sec; $t = 16$ min. **(a)** Precipitation during diffusion. Curve 1 is the ideal (*erfc*) distribution; curve 2 is the precipitated profile $C_p$. Curve 3, the total-phosphorus (radio-tracer) profile, is also the sum of curves 1 and 2. Curve 4, the electrically-active phosphorus profile, is obtained by subtracting 2 from 1. The shaded area is the deviation of the total-phosphorus distribution from the ideal, and changes sign at point A, the intersection of curves 3 and 4. The curves 3 and 4 are expected to be coincident below point A, as shown schematically in the illustration. **(b)** Precipitation during quenching (precipitation time, 2 sec). Curve 1 is the ideal (*erfc*) distribution; curve 2 is the precipitation profile, $C_p$. Also shown is the dislocation density, $L$.

$5 \times 10^{-13}$ cm²/sec for diffusion at 1050°C. Diffusion is assumed to take place over a period of 16 minutes. The hypothetical phosphorus diffusion profile obviously cannot represent impurities in true solution. It represents the sum total of the impurities in solid solution and impurities (not in true solution) *prior* to their transport to the dislocations. We will therefore use this hypothetical curve only as a measure of excess concentration under the influence of dislocations.

Using Eq. (4), values of $W$ for various dislocation densities under the diffusion conditions specified above were obtained and are given in Table 1. Table 2 gives the values of $C_p$ (atoms/cm³) for various dislocation densities $L$ and excess concentrations. The excess concentration should be remembered as the concentration in excess of the solid solubility limit. The precipitated profiles $C_p(x)$ for the dislocation distribution (given by curve 2 in Fig. 2) are shown in Fig. 8 for diffusion with $C_s = 10^{21}$ atoms/cm³.

The distribution of the electrically active phosphorus is obtained by subtracting the precipitated profile $C_p$ (curve 2) from the ideal *erfc*-distribution (curve 1). The total-phosphorus profile is represented by curve 3, which was

**Table 1.** Values of precipitated solute fraction $W$ for various dislocation densities.*

| *Dislocation density, L, cm/cm³* | $Dt/r_s^2$ | *Precipitated fraction, W* |
|---|---|---|
| $5 \times 10^9$ | 7.9 | 0.98 |
| $10^9$ | 1.58 | 0.71 |
| $10^8$ | 0.186 | 0.10 |
| $10^7$ | 0.0158 | 0.005 |
| $10^6$ | 0.00186 | 0.0002 |

* Diffusion conditions: $D = 5 \times 10^{-13}$ cm²/sec; $T = 1050$°C; $t = 16$ min.

obtained as the sum of curve 1 and curve 2. Since the assumption is made that the dislocations only redistribute the total amount of the material entering the wafer after time $t$, then if an area is added to curve 1 near the dislocated surface, an equivalent area must be subtracted from point A onwards as shown in Fig. 8a. Consequently a shallower junction depth, due to depletion of the impurity flux in the dislocation-free region of the diffusion zone, is expected. Such an effect is actually encountered in practice.[15] The curves 3 and 4 from point A onwards are shown only schematically in Fig. 8a and represent the electrical and the total phosphorus profiles simultaneously.

• *Precipitation during quenching*

It will be appropriate at this stage to explore the consequences of the mechanism of precipitation during quenching. We are, however, required to assume the highest possible value of the solid-solubility limit data,[9] *viz.* $\approx 10^{21}$ atoms/cm³ at 1050°C, in order to obtain some significant values of $C_p$. This diffusion profile is then expected to follow the ideal *erfc* distribution with $C_s = 10^{21}$ atoms/cm³ (see Fig. 8b) prior to removal of the diffused wafer from the diffusion furnace. The precipitation time will be taken to be 2 seconds, during which the wafer cools down to 850°C according to our observations. At this temperature the atomic movement is frozen considerably and the reduced solid-solubility limit is $3 \times 10^{20}$ atoms/cm³. All the phosphorus concentrations in excess of this solubility limit will be under the influence of the dislocation field.

We must use the same diffusion constant as in previous calculations, *viz.* $5 \times 10^{-13}$ cm²/sec at 1050°C, since this constant is valid for all the phosphorus distributions following the ideal *erfc* functions. It is also known that the values of $D$ decay rapidly with the temperature. We will not consider this, however, since it will be informative to know how large an amount of precipitation should be expected under conditions that may exaggerate the precipitation effects.

The dislocation-precipitation curve $C_p$ vs. $x$ obtained for the precipitation during quenching is shown in Fig. 8b. The procedure used to obtain this curve is identical with that used for obtaining precipitation during diffusion. Figure 8b shows that the amounts of precipitation during quenching were very small and consequently do not significantly affect the ideal *erfc* functions.

It may be argued that the value of $D$ used in calculating the precipitated fraction $W$ is rather small. Tannenbaum, for example, has shown the concentration dependence of $D$, which increases from $5 \times 10^{-13}$ to $10^{-11}$ cm²/sec for the phosphorus concentration range $10^{20}$ to $10^{21}$ atoms/cc. The value of $D$ could be as large as $10^{-11}$ cm²/sec, but it does not seem justifiable to use so large a value here, for the following reasons: (1) The high values of $D$ are calculated from non-ideal experimental profiles. Our objective is to derive the non-ideal profiles from the ideal *erfc* distribution. (2) The experimental ideal profiles give the concentration-independent value of $D \approx 5 \times 10^{-13}$ cm²/sec. (3) The use of $D = 10^{-11}$ cm²/sec in order to obtain the hypothetical curve 1 in Fig. 8a, gives junctions considerably deeper than are experimentally obtained. (4) The high value of $D = 10^{-11}$ cm²/sec at phosphorus concentration $10^{21}$ atoms/cm³ is based upon the Boltzmann transformation of the radio-tracer profiles. The transformation technique assumes that $x$ and $t$ are involved separately, i.e., can be expressed as a single parameter $\eta = x/2(t)^{\frac{1}{2}}$. This is obviously not true when precipitation effects are involved in a diffusion profile.

When calculations are deductively compared with experiment then, it seems more appropriate to use the lower value of $D$. Experimental information in correlation of the larger values is not available at present, and such calculations would be speculative in this discussion. The use of the larger values, however, cannot be ruled out. An impurity acted upon by the strain field of a dislocation may diffuse considerably faster.

In summary, therefore, we shall state that for $D = 5 \times 10^{-13}$ cm²/sec, the effects of precipitation during quenching do not cause significant deviation from the ideal diffusion profile.

## Discussion

The major consequences of the dislocation precipitation occurring during diffusion as seen from Fig. 8a are:

(a) There exists a large difference between the electrically active impurity profile and the total phosphorus profile.

(b) Impurity profiles measured by electrical measurements should indicate almost a flat curve near the surface where the dislocation density is the highest.

(c) There should be a certain amount of "pile-up" of the total phosphorus near the surface.

**Table 2.** Values of $C_p$.

| *Dislocation density, L,* cm/cm³ | *Excess concentration, atoms/cm³* | | | | | |
|---|---|---|---|---|---|---|
| | $5 \times 10^{21}$ | $2.5 \times 10^{21}$ | $10^{21}$ | $5 \times 10^{20}$ | $2.5 \times 10^{20}$ | $10^{20}$ |
| $5 \times 10^{9}$ | $4.7 \times 10^{21}$ | $2.4 \times 10^{21}$ | $9.4 \times 10^{20}$ | $4.7 \times 10^{20}$ | $2.4 \times 10^{20}$ | $9.4 \times 10^{19}$ |
| $10^{9}$ | $3.5 \times 10^{21}$ | $1.7 \times 10^{21}$ | $6.9 \times 10^{20}$ | $3.5 \times 10^{20}$ | $1.7 \times 10^{20}$ | $6.9 \times 10^{19}$ |
| $10^{9}$ | $5.0 \times 10^{19}$ | $2.5 \times 10^{19}$ | $1.0 \times 10^{19}$ | $5.0 \times 10^{18}$ | $2.5 \times 10^{18}$ | $1.0 \times 10^{18}$ |
| $10^{7}$ | $2.5 \times 10^{19}$ | $1.3 \times 10^{19}$ | $5.0 \times 10^{18}$ | $2.5 \times 10^{18}$ | $1.3 \times 10^{17}$ | $5.1 \times 10^{16}$ |
| $10^{6}$ | $1.0 \times 10^{18}$ | $5.0 \times 10^{17}$ | $2.0 \times 10^{17}$ | $1.0 \times 10^{17}$ | $5.0 \times 10^{17}$ | $2.0 \times 10^{16}$ |

All of these characteristics seem to be consistent with the general features observed in the experimental curves shown in Fig. 1. According to the assumptions of this model, diffusion of phosphorus with $C_s = 2 \times 10^{20}$ atoms/cm³ or less should not cause any deviation from the expected ideal distribution. This is also observed in practice.[1]

It is possible that some of the assumptions made for the purpose of calculating the profile $C_p$ could have been responsible for exaggerating the dislocation effects. Particular mention should be made in this respect of the assumptions (3) and (5) noted in the section, *Results.* We arbitrarily assumed in (3) a static distribution of dislocations from the beginning of the diffusion process. In reality, the dispersion of dislocations into the interior should follow the diffusion in order to compensate for the strains continuously being created by the inward-diffusing atoms. According to Prussin, a much deeper penetration of dislocations is expected, as shown in Fig. 2. The solute pinning is primarily responsible for the observed shallow distribution of the dislocations. In the absence of sufficient experimental knowledge regarding the kinetics of the dislocation dispersion inside the diffusion zone, it was decided to postulate the existence of the dislocation distribution given by curve 2 in Fig. 2 from the very beginning of the diffusion. In doing this, we assumed the same diffusion time $t$ for the precipitation at all the levels of the dislocation profile. This could have caused a higher estimate of the values of $W$, particularly for the lower end of the dislocation distribution. This should not, however, affect our calculations seriously since the major contribution to the profile $C_p$ comes from the high density of dislocations near the surface. The dislocations near the surface should be involved in accumulating the solute almost all the time during diffusion.

Assumption (5) also needs some explanation. Competition for solute between slices (Fig. 7) was neglected since electron microscope observations have indicated that the majority of dislocations lie in planes parallel to the surface of diffusion. Also, according to the Prussin model of diffusion-induced dislocations, the dislocations created during diffusion must lie in the planes parallel to the diffusion plane for stress relief, and their Burgers vectors must be in those same planes. For these reasons, the cross-connections between dislocation nets lying on different planes parallel to the diffusion surface were not considered to be important in the evaluation of $C_p$. In addition, not much is known of the density and distributions of these cross-connections. From this, it will be apparent that we have neglected "pipe diffusion" along these cross-connecting dislocations with a lengthwise concentration gradient. (It should be borne in mind that the dislocation precipitation phenomenon and "pipe diffusion" along dislocations are two distinctly different processes.) These reasons, then, are used to justify the fifth assumption and the scheme of evaluation of $C_p$ as illustrated in Fig. 7.

It should be re-emphasized that the term "electrically active phosphorus" is equivalent to the total phosphorus in true-solid solution. This also implies that the $C_s$ value as obtained from the electrical profile should not exceed the solid solubility limit. The curve 4 in Fig. 8b does approach this condition. If the value of $C_s$ obtained from the electrical curve does not exactly correspond to the solid solubility limit, it means only that we have not been able to precisely calculate and subtract from curve 1 the exact amount of phosphorus that is out of true solution.

In conclusion, therefore, it can be stated that the proposed dislocation-precipitation model can adequately explain the major features of the deviations of the phosphorus-impurity profiles from ideal ones. The nearly flat curve of the concentration of the electrically active phosphorus versus $x$ near the surface has been interpreted by Kooi[10] as an indication of the presence of interstitial states which diffuse very quickly. The calculated amounts of precipitation on dislocations as shown here and the corresponding evidence (Fig. 3) account for the actual experimental differences between the electrical and the

radio-tracer profiles. Therefore, it is not necessary to assume the existence of an extra-fast interstitial diffusion component. The phenomenon of partial ionization of phosphorus has also been shown by researchers[1] to be inadequate to explain the flatness of the electrical profile near the surface. Thus the proposed dislocation precipitation model is perhaps the best explanation for the large difference between the electrical and the total phosphorus profiles.

Beyond the precipitation of impurities on dislocations, there exists general precipitation of phosphorus in the silicon matrix, which could also make a substantial contribution to the precipitated profile $C_p$. However, it has not yet been possible to assess this effect quantitatively.

## Acknowledgments

The authors thank M. Duffy and W. Armstrong for very helpful discussions. They must also thank B. Masters and E. Schneider for the radio-tracer measurements.

## References

1. E. Tannenbaum, *Solid State Elect.* **2**, 123 (1961).
2. D. N. Mikhailova and I. D. Kasabov, *Sov. Phys. Solid State* **4**, 1228 (1962).
3. T. J. Lachapelle, *Final Report, USAF Contract 18(603)-117 (1957)*.
4. W. Shockley, *J. Appl. Phys.* **32**, 1402 (1961).
5. J. C. Irvin, *Bell System Tech. J.* **41**, 387 (1962).
6. M. L. Joshi and F. Wilhelm, *J. Electrochem. Soc.* **112**, 185 (1965).
7. S. Prussin, *J. Appl. Phys.* **32**, 1876 (1961).
8. M. L. Joshi, *J. Electrochem. Soc.* **112**, 912 (1965).
9. F. A. Trumbore, *Bell System Tech. J.* **39**, 205 (1960).
10. E. Kooi, *J. Electrochem. Soc.* **111**, 1383 (1964).
11. N. K. Abrikosov, V. H. Glazov, and L. Chen-Yiian, *Russ. Journ. Inorg. Chem.* **7**, 429 (1962).
12. A. H. Cottrell, *Report on the Strength of Solids* (London: Physical Society), p. 30 (1948).
13. A. H. Cottrell and B. A. Bilby, *Proc. Phys. Soc.* **62, I-A**, 49 (1949).
14. F. S. Ham, *J. Appl. Phys.* **10**, 915 (1959).
15. M. C. Duffy, F. Barson, and G. H. Schwuttke, "High Concentration Phosphorus Diffusion in Silicon," to be published.

*Received March 15, 1966.*